Rydberg-atom photoionization with and without the single-n manifold approximation

R. Parzyński, M. Sobczak, and A. Wójcik
Faculty of Physics, A. Mickiewicz University, Umultowska 85, 61-614 Poznań, Poland

(Received 10 July 2000; revised manuscript received 1 February 2001; published 16 May 2001)

In a wide basis of bound hydrogenic states ($20 \leqslant n \leqslant 80, l \leqslant 29$), we simulate redistribution of the initial 50s state population by a nonresonant, optical-frequency pulse of the strength at which Rydberg-to-Rydberg Rabi frequencies exceed the pulse frequency. A small transient flow of the population out of the 50l manifold ($l = 0,1,2,3,...$) is observed and the effect of this $n \neq 50$ redistribution on the formation of the photoionization signal from Rydberg states is calculated in the limit of weak bound-free coupling. This $n \neq 50$ redistribution is found to totally cancel the predictions of the single-n manifold approximation ($n = 50$ in this case) in photoionization.

DOI: 10.1103/PhysRevA.63.063413 PACS number(s): 32.80.Rm, 42.50.Hz

What is referred to as the single-n manifold approximation was introduced by Corless and Stroud [1] in their study of selective excitation by an optical-frequency pulse of the n_0p hydrogenic state of $n_0 \gg 1$ followed by optical mixing of this state with other angular-momentum l states within the n_0 level only. All other $n \neq n_0$ levels were omitted in this study on the basis of much smaller $\Delta n \neq 0$ dipole transition moments than the $\Delta n = 0$ ones. This single $n = n_0$ manifold approximation resulted in an effective transient mixing of a number of different l states, of both parities, with only odd-parity states left populated after the pulse. According to [1], the condition for the mixing to occur is a sufficient strength of the pulse ensuring that the $n_0, l \rightarrow n_0, l+1$ Rabi frequency exceeds the optical frequency of the pulse. For a high enough n_0, this strength condition needs rather low intensities allowing the excitation of the n_0p state to be treated perturbatively as, in fact, it was in the study of Corless and Stroud. With the same perturbative treatment of the excitation step, Muller and Noordam [2] argued within an analytically solvable model that the inclusion of off-resonant $n \neq n_0$ states, lying outside the pulse bandwidth, leads to suppression of the l-state mixing by an optical pulse and thus zero population in odd, $l > 1$, states after the pulse. In a different coupling scheme of Mecking and Lambropoulos [3], with two time-separate pulses, one of optical frequency weakly exciting a p Rydberg radial wave packet around $n_0 = 30$ and the other of infrared frequency mixing different-l Rydberg states, nonzero population in odd states up to $l = 7$ was reported, likely due to the vicinity of the n_0 to a lower-state resonance, while no l-state mixing was observed in the case of optical frequencies. On the other hand, Nilsen and Hansen [4] showed that, beyond the scope of applicability of the perturbation theory for the excitation step, the inclusion of $n \neq n_0$ Rydberg states does not automatically destroy the optical mixing of l states and thus the population in odd, $l > 1$, high-n Rydberg states after the pulse.

The present paper concerns a different process, which starts from a high n_0s state of $n_0 \gg 1$, as opposed to the 1s or 2s initial states of the cases described above. The other difference is that the pulse redistributing the initial population is off-resonant. We shall show that, although the transient redistribution prefers the n_0 manifold, much smaller transient population of other $n \neq n_0$ manifolds plays a crucial role when calculating perturbatively the photoionization outcome from Rydberg states. The overall effect of $n \neq n_0$ manifolds will be shown to completely cancel what the single $n = n_0$ manifold approximation predicts in photoionization, as long as the photoionization step can be treated by the perturbation theory. To a great extent, this result is obtained numerically without approximating the Rydberg-state world by any other structure, e.g., of the equidistant, infinite, Bixon-Joertner type. It confirms our earlier supposition [5] formulated on the basis of rough analytical calculations with the Bixon-Joertner modeling of the Rydberg-state space.

For proof, the 50s state hydrogen atom is exposed to a laser pulse $\varepsilon(t) = \varepsilon_0 f(t)\cos(\omega t)$ of the $f(t) = \sin^2(\pi t/t_f)$ or $f(t) = 1$ envelope, 620-nm wavelength ($\omega = 0.0735$ a.u.), linear polarization along the z axis ($\Delta m = 0$), and duration t_f equal to 10 optical cycles ($\omega t_f = \tau_f = 20\pi$). The wavelength chosen prevents a resonance with any lower-lying state, while the peak intensity of the pulse is assumed to amount to 10^9 W/cm^2 only. Despite this moderate intensity, the 50s-50p Rydberg-to-Rydberg Rabi frequency exceeds the optical frequency by as much as a factor of 5.6 due to a large transition dipole moment [$\Omega/\omega = 5.6$, $\Omega = (e\varepsilon_0/\hbar) z_{50s,50p}$]. For this pulse, we calculate numerically transient redistribution of the initial 50s population over different Rydberg states, neglecting ionization losses of the bound-state population as a minor effect at the intensity and wavelength considered. This means that we solve in the discrete-state subspace the Schrödinger-type equation for the population amplitudes c_j, i.e.,

$$dc_j/d\tau = i f(\tau)\cos(\tau)\sum_{j'} \Omega_{jj'} c_{j'} \exp(i\omega_{jj'}\tau), \qquad (1)$$

where $0 \leqslant \tau = \omega t \leqslant \tau_f = 20\pi$, while $\Omega_{jj'}$ and $\omega_{jj'}$ are given in units of ω. The states forming the basis for the numerical integration were taken as those of the principal quantum numbers $n_{\min} \leqslant n \leqslant n_{\max}$, where $n_{\min} \geqslant 20$ and $n_{\max} \leqslant 80$, and of the angular quantum numbers truncated at $l = 29$. So we worked with 61 different-n manifolds in the extreme case, spaced around the $n_0 = 50$ manifold, with a given-n manifold being a chain of states differing in l only. The calculated transient populations, $|c_j(\tau)|^2$, exhibited fast variations,

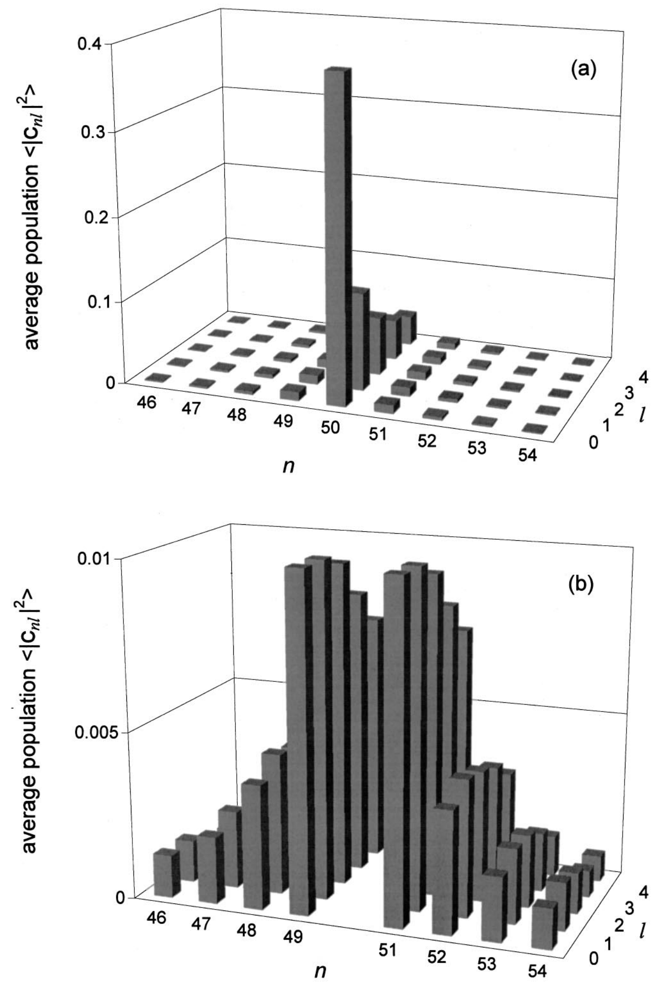

FIG. 1. Time-averaged populations in different nl states obtained from the model with 61 manifolds ($20\leqslant n\leqslant 80$) and $f(\tau)=\sin^2(\tau/20)$ pulse. In (b), the dominant $50l$ populations were removed to show better the redistribution over $n\neq 50$ states.

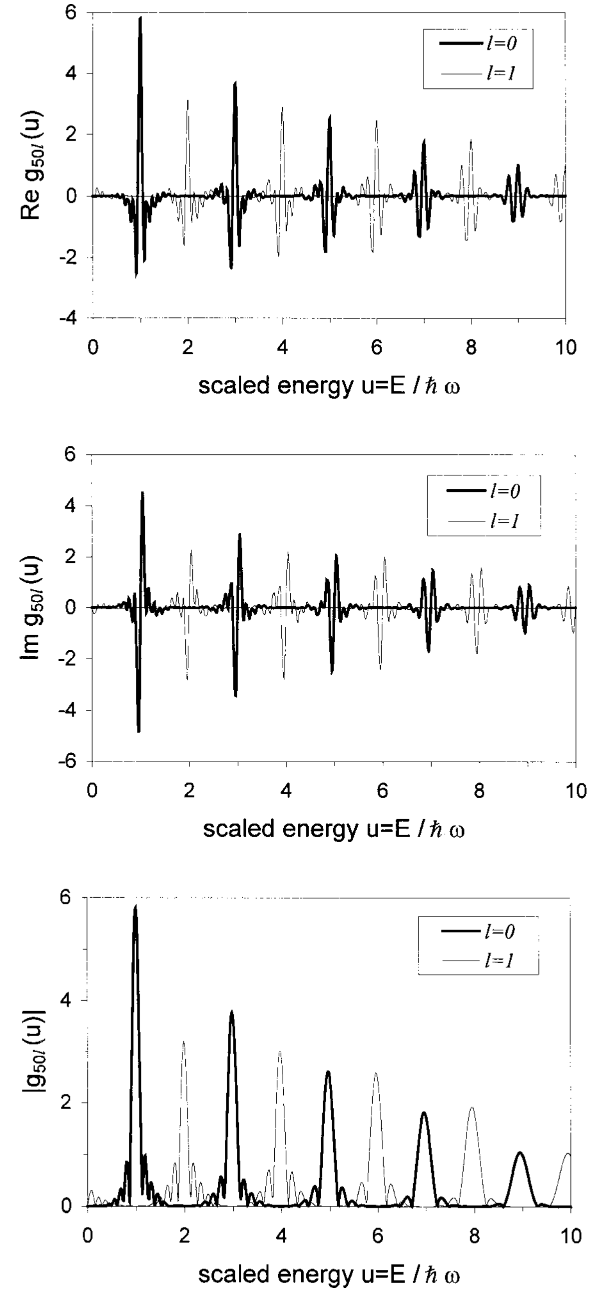

FIG. 2. The spectra $g_{50l}(u)=\int_0^{20\pi}\sin^2(\tau/20)\cos(\tau)b_{50l}(\tau)e^{iu\tau}d\tau$ obtained from the model with 61 manifolds ($20\leqslant n\leqslant 80$).

even in a time scale of the order of an optical period, so we decided to visualize them as time-averaged over the pulse length, i.e., $\langle|c_{nl}|^2\rangle=(1/\tau_f)\int_0^{\tau_f}|c_{nl}|^2d\tau$. Figure 1 shows such average populations obtained in the basis of 61 manifolds with an $f(\tau)=\sin^2(\tau/20)$ pulse. This figure says that, on average, the majority of the population does reside in the $n_0=50$ manifold, i.e., that to which the initial state belongs, most likely due to larger $\Delta n=0$ dipole transition moments than the $\Delta n\neq 0$ ones. Thus, we could be inclined to treat the $n=50$ manifold as the only essential one and neglect all other ($n\neq 50$) manifolds as getting much less population during the laser pulse. In the following, we shall prove that the neglect of the $n\neq 50$ manifolds, as is the essence of the single-n manifold approximation, results in extremely wrong predictions for photoionization.

As a small perturber to the Rydberg-state redistribution, the photoionization to the atomic continuum of energy E is calculated perturbatively from the above discrete amplitudes $c_j=b_j\exp(i\omega_j\tau)$. In this approach, the photoionization amplitude $c_E=c(u=E/\hbar\omega)$ is to be found from

$$c(u)=i\frac{e\varepsilon_0}{\hbar\omega}\sum_j z_j^E g_j(u),\quad g_j(u)=\int_0^{\tau_f}g_j(\tau)\exp(iu\tau)d\tau, \tag{2}$$

where $g_j(u)$ is a Fourier-like, finite-time, $\tau\to u$ transform of $g_j(\tau)=f(\tau)\cos(\tau)b_j(\tau)$, while $z_j^E=\langle E|z|j\rangle$ is the standard bound-free dipole matrix element. The analysis of $g_j(u)$ versus the normalized photoelectron energy $u=E/\hbar\omega$ exhibits a quasidiscrete structure of $g_j(u)$ irrespective of how many n manifolds is taken into account when calculating b_j. In Fig. 2, we show exemplifying $g_j(u)$ spectra obtained for the $50s$ and $50p$ states, respectively, from the model including 61 manifolds ($20 \leqslant n \leqslant 80$) and the $\sin^2(\tau/20)$ pulse. We observe trains of well-pronounced structures localized around integer u, i.e., $E \simeq N\hbar\omega$, where N is either odd or even depending on the parity (l_j) of the Rydberg state coupled to the continuum. With our choice of the initial state ($50s$), N and l_j are found to be of opposite parity in accordance with the multiphoton selection rules.

The quasidiscreteness of $g_j(u)$ allows us to write $g_j(u) = \Sigma_N g_j(u_N)$, where N is either odd or even, with $(N-1) \leqslant u_N \leqslant (N+1)$ being a piece of the u axis around a given peak in $|g_j(u)|$. Within a given-N peak, we treat the bound-free matrix element z_J^E as E-independent and take it as that for $E = E(N) \simeq N\hbar\omega$. This results in the splitting of the photoionization amplitude $c(u)$ into a number of partial amplitudes, $c(u) = \Sigma_N c(u_N)$, with $c(u_N)$ obtained from the above-defined $c(u)$ by replacing $E \to E(N)$ and $u \to u_N$. The photoionization probability to the Nth peak, $W^{(N)}$, is then

$$W^{(N)} = \rho(E(N))\hbar\omega \int_{N-1}^{N+1} |c(u_N)|^2 du_N$$
$$= 2\rho(E(N)) \frac{(e\varepsilon_0)^2}{\hbar\omega} \sum_{jj'} z_j^{E(N)} (z_{j'}^{E(N)})^*$$
$$\times \int_0^{\tau_f} d\tau\, g_j(\tau) e^{iN\tau} \int_0^{\tau_f} d\tau'\, g_{j'}^*(\tau') e^{-iN\tau'} \frac{\sin(\tau-\tau')}{\tau-\tau'}, \qquad (3)$$

where $\rho(E(N))$ is the photoelectron-state density around $E(N) = N\hbar\omega$. The use of the standard partial-wave representation for the photoelectron state $|E(N)>$ [5] converts Eq. (3) into

$$W^{(N)} = \frac{2\pi}{\hbar} t_f \rho(E(N))(e\varepsilon_0)^2$$
$$\times \sum_{l,l' \geqslant |m|} Z_{ll'}^{(N)} Y_{l,m}(\theta,\phi) Y_{l',m}^*(\theta,\phi), \qquad (4)$$

where the summation runs over the photoelectron l numbers of the same parity as that of N, and θ, ϕ are the angles of the photoelectron ejection in the coordinate system with θ measured with respect to the direction of light polarization ($\|z$). In the above, the $Z_{ll'}^{(N)}$ expansion coefficients are

$$Z_{ll'}^{(N)} = \frac{1}{\pi\tau_f} \beta_l^*(E(N)) \beta_{l'}(E(N)) \int_0^{\tau_f} d\tau\, f(\tau) \cos(\tau) B_l^{(N)}(\tau)$$
$$\times e^{iN\tau} \int_0^{\tau_f} d\tau'\, f(\tau') \cos(\tau')$$
$$\times [B_{l'}^{(N)}(\tau')]^* e^{-iN\tau'} \frac{\sin(\tau-\tau')}{\tau-\tau'}, \qquad (5)$$

where

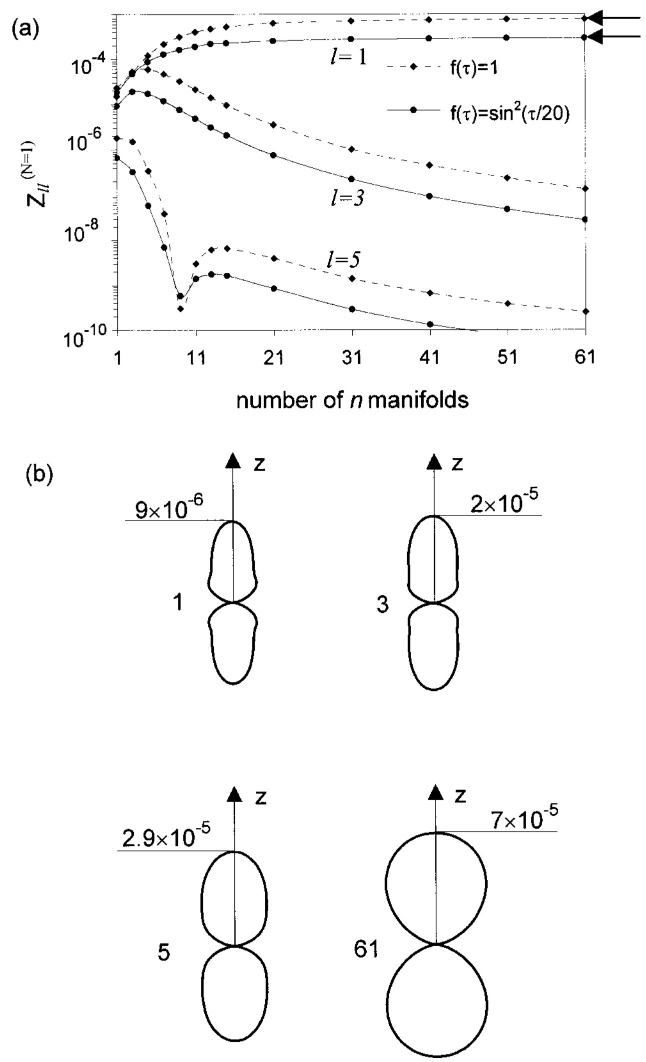

FIG. 3. The $Z_{ll}^{(1)}$ coefficients vs the number of n manifolds included in calculations (a), and the resulting photoelectron angular distributions ($\Sigma_{ll'} Z_{ll'}^{(1)} Y_{l0} Y_{l'0}^*$) for the $\sin^2(\tau/20)$ pulse vs this number (b). In (a), the arrows on the right-hand side point to the values (0.0008 and 0.0003, respectively) provided by the standard model with only the $50s$ Rydberg state and p continuum included.

$$B_l^{(N)}(\tau) = \sum_j z_{n_j, l_j, m}^{E(N), l, m} b_j(\tau)$$
$$= \sum_{\Delta=\pm1} \sum_{n>l+\Delta} z_{n, l+\Delta, m}^{E(N), l, m} b_{n, l+\Delta, m}(\tau), \qquad (6)$$

while $\beta_l(E(N)) = i^1 [\Gamma(l+1+i/y(N))/\Gamma(l+1-i/y(N))]^{1/2}$ is a phase shift of an lth partial wave, with $y(N) = [2E(N)]^{1/2}$ and $E(N)$ given in a.u. In the case of interest, $m=0$ due to our choice of the initial state ($50s$) and polarization of the light pulse (linear).

The numerically found bound-state amplitudes $b_j = c_j \exp(-i\omega_j\tau)$ were used to perform numerically the double time integration in Eq. (5), for the $f(\tau) = \sin^2(\tau/20)$ and $f(\tau) = 1$ pulses, both of 10 optical cycle length at $\omega = 0.0735$ a.u. The calculation of a given $Z_{ll'}^{(N)}$ coefficient was performed for the pulse strength $\Omega/\omega = 5.6$ in its dependence on the number of n manifolds included. We mean that the single-n manifold model is the one including the $50l$ chain ($l = 0,1,2,...$) only, i.e., the chain distinguished by the initial-state choice ($50s$). For example, the three-n manifold model is the one including also the $49l$ and $51l$ chains, the five-n manifold model includes additionally the $48l$ and $52l$ chains, and so on. So, a model with $k+1$ (k even) different manifolds means that, in addition to the $50l$ chain, we also take into account $k/2$ successive chains lying above and $k/2$ successive chains lying below the $50l$ chain $[50-(k/2) \leqslant n \leqslant 50+(k/2)]$. In Fig. 3(a), we show the variation of the most important diagonal $Z_{ll}^{(1)}$ coefficients, determining the ionization to the first photoelectron energy peak $[N=1,\ E(N) \simeq \hbar\omega]$, when increasing the number of n manifolds. The solid lines correspond to the $f(\tau) = \sin^2(\tau/20)$ pulse, while the dotted lines are the results for the $f(\tau) = 1$ pulse, i.e., the square pulse. The observed strong dependence of the $Z_{ll}^{(1)}$ coefficients on the number of n manifolds, particularly for the number of manifolds in the range between 1 and 21, undermines the photoionization results obtained within the model with only a single-n or a few-n manifolds included. It is necessary to include many n manifolds to reach convergence of the results [3]. Figure 3(b) shows the effect of the number of n manifolds included on the photoelectron angular distributions produced by the $f(\tau) = \sin^2(\tau/20)$ pulse in the first energy peak ($N=1$). The specific lobes in the angular distributions at $\theta \simeq 63°$, as seen in the case of a small number of n manifolds included, and generated by the Y_{30} spherical harmonic, are completely canceled when the number of n manifolds is sufficiently increased.

To conclude, we indicate by the horizontal arrows in Fig. 3(a) the $Z_{11}^{(1)}$ values obtained from the standard photoionization model, consisting of only the initial $50s$ and final p continuum states, weakly coupled to each other, with no other Rydberg states taken into account. These values were found by retaining in $B_1^{(1)}(\tau)$ the $50s$ state only and setting $b_{50s}(\tau) = 1$ in accordance with the perturbative treatment of the bound-free transition. The indicated values 0.0008 and 0.0003, respectively, seem to be the asymptotic limits approached by the two uppermost curves in Fig. 3(a) when increasing the number of n manifolds. This would suggest that, in weak photoionization of the $50s$ state by a nonresonant optical pulse, the effect of $n \neq 50$ manifolds is to cancel all deviations, produced by the single $n=50$ manifold approximation, from the perturbative results. The obtained result is a spectacular effect of quantum interferences and to some extent it is a photoionization analog to the result of Muller and Noordan [2] on suppression of high-harmonic generation in an extended photoexcitation model of Corless and Stroud, i.e., including a number of n manifolds instead of one.

This research was made possible thanks to the support from the Polish Committee for Scientific Research under Grant No. 2 PO3B 026 19.

[1] J. D. Corless and C. R. Stroud, Jr., Phys. Rev. Lett. **79**, 637 (1997).
[2] H. G. Muller and L. D. Noordam, Phys. Rev. Lett. **82**, 5024 (1999); **85**, 899 (2000); see also a comment by L. B. Madsen, *ibid.* **85**, 898 (2000).
[3] B. S. Mecking and P. Lambropoulos, Phys. Rev. Lett. **83**, 1743 (1999).
[4] H. M. Nilsen and J. P. Hansen, Phys. Rev. A **63**, 011405(R) (2000); see also H. M. Nilsen, J. P. Hansen, S. Selstø, and L. B. Madsen, J. Phys. B **32**, 4995 (1999).
[5] R. Parzyński, M. Sobczak, and A. Wójcik, Phys. Rev. A **61**, 023413 (2000); A. Wójcik, *ibid.* **63**, 023412 (2001).